Available online at www.sciencedirect.com
ScienceDirect
Microelectronic Engineering 85 (2008) 110–114
MICROELECTRONIC ENGINEERING
www.elsevier.com/locate/mee

Effect of size and plasma treatment and the application of Weibull distribution on the breakdown of PECVD SiN_x MIM capacitors

Chia-Cheng Ho [a], Bi-Shiou Chiou [a,b,*]

[a] Department of Electronics Engineering and Institute of Electronics, National Chiao Tung University, Hsinchu, Taiwan
[b] Innovative Packaging Research Center, National Chiao Tung University, Hsinchu, Taiwan

Received 27 September 2006; received in revised form 2 February 2007; accepted 18 April 2007
Available online 16 May 2007

Abstract

The dielectric breakdown field is one of the important concerns for device reliability. The breakdown of dielectric is originated at a fatal flaw that grows to cause failure and can be explained by the weakest-link theory. In this study, metal-insulator-metal (MIM) capacitors with plasma enhanced chemical vapor deposited (PECVD) SiN_x are prepared. Ammonia (NH_3) plasmas are applied after the deposition of the dielectric SiN_x. The Weibull distribution function, which is based on the weakest-link theory, is employed to analyze the effect of the electrode area as well as the plasma treatment on the breakdown of the MIM capacitors. The time dependent dielectric breakdown testing indicates a decrease in both the leakage current and the lifetime of the MIM capacitors treated with plasma. Possible dielectric degradation mechanisms are explored.

Keywords: Weibull distribution; Weakest-link theory; Plasma treatment; Electric field

1. Introduction

When an electron current passes through the dielectric layer of a capacitors, defects such as electron traps, interface states, etc., gradually build up in the dielectric until a critical defect density is reached where the dielectric suddenly and destructively breaks down. The dielectric breakdown field and time dependent dielectric breakdown (TDDB) are main factors of the important concerns for device reliability especially in deep submicron technology as device is scaled down [1]. It is reported that when the oxide SiO_2 is thicker than 5 nm, hard breakdown caused by hot-hole injection is its major failure, the breakdown mechanisms were generally accepted to be charge trapping in the oxide [2], and a critical defect density of around 5×10^{13} cm^{-2} was reported [3]. The critical defect for breakdown shows a strong decrease with thickness below about 5 nm, and then becomes constant below 3 nm. The critical defect density is explained by the formation of a percolation path of defects across the oxide and the formation of the breakdown path [4–7]. Besides, for ultrathin oxide (1.4–2.2 nm), the location of the damaged region is relevant to the oxide breakdown [8,9]. Allers [10] derived the physical model offers the consistent description of the metal-insulator-metal (MIM) capacitors with SiN_x and shows the relations of the dielectric breakdown of SiN_x and the charge of breakdown [10]. However, although there have been many works related to the thickness effect of oxide breakdown. Very few work reports on the area effect on the dielectric breakdown.

This is a continuing research and our previous work reveals that plasma treatment eliminates the dispersive behavior and electrical hysteresis of the SiN_x MIM capac-

---

[*] Corresponding author. Address: Department of Electronics Engineering and Institute of Electronics, National Chiao Tung University, Hsinchu, Taiwan.
E-mail address: bschiou@mail.nctu.edu.tw (B.-S. Chiou).

0167-9317/$ - see front matter © 2007 Elsevier B.V. All rights reserved.
doi:10.1016/j.mee.2007.04.151

itors. Besides, the leakage current density of SiN_x MIM capacitors decreases due to the decrease of the trap density after plasma treatment [11]. In this study, MIM capacitors with plasma enhanced chemical vapor deposited (PECVD) SiN_x were fabricated. Ammonia (NH_3) plasma was applied to the as-deposited SiN_x capacitor, before deposition of the upper electrode. The effects of electrode area and plasma treatment on the breakdown strength of the dielectric are investigated using Weibull distribution. Finally, we describe the TDDB characterizations of the as-deposited and plasma-treated SiN_x capacitors, and the breakdown electric fields for 10 years lifetime are represented in this paper.

2. Experimental procedures

Four inch diameter p-type (100) Si wafers with nominal resistivity of 1–10 Ω-cm were used as substrate. After standard RCA cleaning process, a 100 nm thick SiO_2 film was grown on the Si substrate. A 100 nm Al film were deposited with thermal evaporation coater onto the SiO_2/Si substrate to serve as the bottom electrode. Silicon nitride (SiN_x) was prepared in this study. While the SiN_x films with a thickness of 50 nm, were deposited with the PECVD system (Multichamber PECVD, STS-MULTIPLEX CLUSTER SYSTEM, England) using a SiH_4/NH_3/N_2 gas mixture. The flow rates of SiH_4, NH_3 and N_2 were 20, 80, and 510 sccm, respectively. Before the deposition of the top electrode, some samples were subjected to plasma treatment. The SiN_x films were treated with SiH_4/NH_3 plasma (the flow rates were 6 and 700 sccm for SiH_4 and NH_3, respectively) for 30 min. Aluminum films (150 nm in thickness) were then deposited as the top electrodes. The electrodes are circular in area.

The electrode areas of capacitors in this study are: 2.37×10^{-3} cm^2 (radius $r = 275$ μm), 1.59×10^{-3} cm^2 ($r = 225$ μm), and 0.96×10^{-4} cm^2 ($r = 175$ μm). The current–voltage (I–V) measurement was carried out with a semiconductor parameter analyzer (HP4155B, Hewlett Packard Co., USA) at 25 °C and 150 °C. The breakdown electric field is defined when the leakage current density exceeds 0.5 A/cm^2. Atomic force microscope (AFM) (NS3a controller with D3100 stage, Veeco Instruments Inc., USA) was employed to measure the surface roughness.

3. Results and discussion

The breakdown of dielectric is thought to originate at a fatal flaw that grows with time. The formation of a weak link threatens the reliability of the electronic components because too defects of critical size will cause failure. The weakest-link theory gives the cumulative probability $F(E)$ that breakdown occurs below electric field (E) for Weibull distribution as [12]:

$$F(E) = 1 - \exp(-E/E_0)^m \tag{1}$$

$$1 - F(E) = \exp(-E/E_0)^m \tag{2}$$

$$\ln(-\ln(1 - F(E))) = m \times \ln(E) - m \times \ln(E_0) \tag{3}$$

where E_0 is the characteristic breakdown field which is the field when 63.2% of capacitors breaks down, and m is called the slope parameter of Weibull distribution. Since m is the Weibull slope of the $\ln[-\ln(1 - F(E))]$ versus $\ln(E)$ plot.

Fig. 1 is the Weibull distribution $\ln(-\ln(1 - F(E)))$ versus $\ln(E)$ plots as a function of electrode area measured at 25 °C and 150 °C of SiN_x MIM capacitors without plasma treatment, while Fig. 2 is that of SiN_x MIM capacitors with plasma treatment. A software named Origin (Microcal Software Inc.) based on minimum chi-square (χ^2) statistics is employed to fit the Weibull distribution $\ln(-\ln(1 - F(E)))$ versus $\ln(E)$ curve. The values of m and E_0 are then evaluated from Figs. 1 and 2 and summarized in Table 1.

As the Weibull distribution function is based on the weakest-link theory, it can be employed to predict the elec-

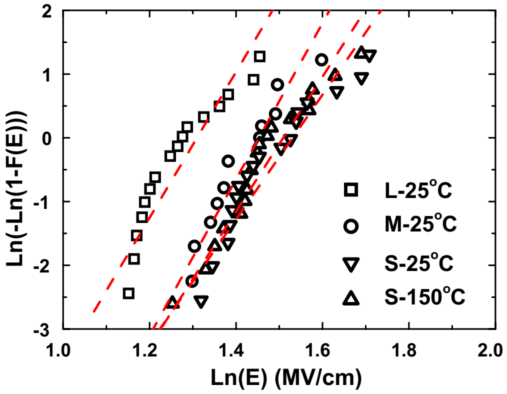

Fig. 1. The Weibull distribution $\ln(-\ln(1 - F(E)))$ versus $\ln(E)$ plots as a function of electrode area measured at 25 °C and 150 °C of as-deposited SiN_x MIM capacitors. Electrode area: L: 2.37×10^{-3} cm^2, M: 1.59×10^{-3} cm^2, S: 9.6×10^{-4} cm^2. Data measured at 25 °C and/or 150 °C.

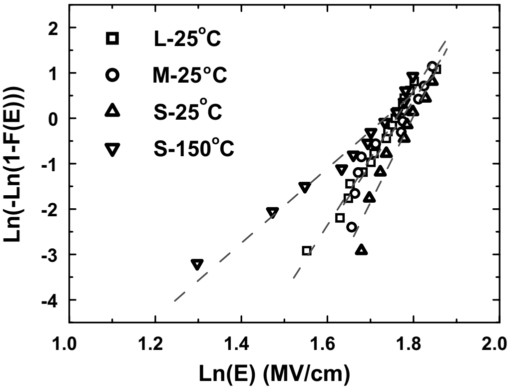

Fig. 2. The Weibull distribution $\ln(-\ln(1 - F(E)))$ versus $\ln(E)$ plots as a function of electrode area measured at 25 °C and 150 °C of plasma treated-SiN_x MIM capacitors. Electrode area: L: 2.37×10^{-3} cm^2, M: 1.59×10^{-3} cm^2, S: 9.6×10^{-4} cm^2. Data measured at 25 °C and/or 150 °C.

Table 1
Weibull slope parameter *m*, the characteristic electric field E_0 and surface roughness of SiN_x MIM capacitors with and without plasma treatment

Electrode area (10^{-3} cm^2)		2.37	1.59	0.96	0.96
Measuring temperature (°C)		25	25	25	150
Without plasma treatment	*M*	11.47	12.28	9.81	10.62
	E_0	3.73	4.29	4.62	4.52
	Surface roughness (RMS)	0.579 nm			
With plasma treatment	*M*	14.86	15.25	19.07	11.51
	E_0	5.79	5.87	5.99	5.63
	Surface roughness (RMS)	0.293 nm			

trode size effect on the breakdown strength of the capacitors. If the dielectric in-between a small portion of the electrode area breaks down, the whole capacitor breaks down. From statistics, if the probability of the dielectric breakdown in-between any one small portion δA of the electrode area is *p*, the probability of the dielectric breakdown between *N* independent small portions of the electrode area is

$$F(E) = 1 - (1 - p)^N \tag{4}$$

$$\ln(-\ln(1 - F(E))) = \ln(N) + \ln(-\ln(1 - p)) \tag{5}$$

Combining Eqs. (3) and (5), one has

$$\begin{aligned} \ln(-\ln(1 - F(E))) &= \ln(N) + \ln(-\ln(1 - p)) \\ &= m \times \ln(E) - m \times \ln(E_0) \end{aligned} \tag{6}$$

The probability *p* of the dielectric breakdown is dependent on both the intrinsic strength of the dielectric and the electric field (*E*) applied. From Eq. (6), one finds that the characteristic breakdown field E_0 is affected by the electrode area, the intrinsic strength of the dielectric, and the electric field applied. The slope *m* and the characteristic breakdown field E_0 were obtained from Figs. 1 and 2 and summarized in Table 1, while they were plotted as a function of electrode area in Fig. 3. The Weibull slope *m* of the individual curves was the measure of the spread in the experimental data. The higher the slope, the smaller is the variation in the measured electrical parameter. When the electrode area increases from A_1 to A_2, the characteristic breakdown field decreases from E_1 to E_2, as described in the following [5].

$$E_1/E_2 = (A_2/A_1)^{1/m} \tag{7}$$

Therefore, the characteristic field E_0 decreases with the increase of the electrode area as predicated from the weakest-link theory and exhibited in Fig. 3. The characteristic field E_0 decreases when the measuring temperature increases from 25 °C to 125 °C. However, no apparent trend is observed between the slope parameter m and the electrode area *A*. Besides, the results of the measurement and simulation with Eq. (7) are shown in Fig. 4 as a plot of the ratios of E_1/E_2 versus the ratio of A_2/A_1. It is obvious the data of the plasma treated SiN_x are fitted better than ones of the as-deposited SiN_x.

The plasma treatment increases the characteristic field E_0 and the slope m. Previous work suggests [11] that ammonia plasma treatment introduces hydrogen atoms into the SiN_x films to form Si–H bonds which reduce the number of silicon dangling bonds (Si DB) in the SiN_x films and decrease the leakage current of the SiN_x capacitors. Besides, Auger depth profiling indicates a slight increase of nitrogen to silicon ratio after plasma treatment in our previous working [11]. On the other hand, the surface roughnesses of SiN_x are smoother after plasma treatment as indicated in Table 1. These may be the reasons why both E_0 and m are improved after plasma bombardment and the ratios of E_1/E_2 versus the ratios of A_2/A_1 can be fitted well by Eq. (7) after plasma bombardment.

Van Delden and van der Wel proposed a degradation mechanism for PECVD SiN_x films in Fig. 5 [13]. The electron-hole recombination breaks the weaker Si–Si and Si–H bonds to form the Si dangling bonds (Si DB) which are singly occupied for the neutral state (Si_3^0). These neutral states trap charge carriers of either sign to form Si_3^+ and Si_3^- centers. The Si_3^+ center may react with N–H to form Si–N and

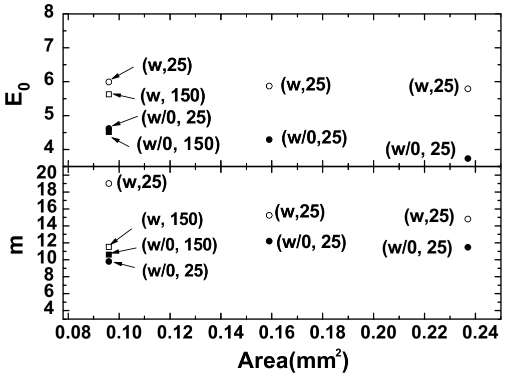

Fig. 3. Weibull slope *m* and characteristic breakdown field E_0 as a function of electrode area of SiN_x MIM capacitors with and without plasma treatment. Sample designation: (w, T) and $(w/0, T)$, where *w*, *w*/0, and *T* stand for with plasma treatment, without plasma treatment, and temperature in °C, respectively.

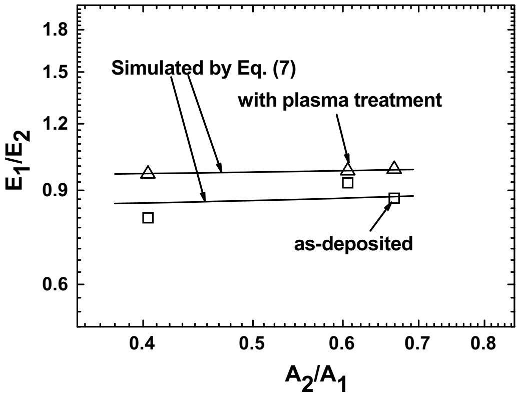

Fig. 4. The results of the measurement and simulation with Eq. (7) as a plot of the ratios of E_1/E_2 versus the ratio of A_2/A_1.

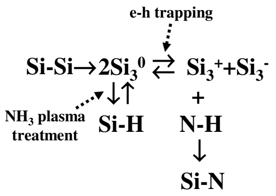

Fig. 5. Schematic representation of the mechanisms describing the Si DB (Si_3^0) during plasma treatment and TDDB test.

leave a net concentration of negatively charged Si_3^- centers. For samples without plasma treatment, the initial increase of the leakage current with time is due to an increase of defects in the band edges. Then, silicon dangling bonds (Si DB) which are occupied for the neutral states (Si_3^0) trap electrons reduce the total current, as shown in Fig. 6. On the other hand, the SiH_4/NH_3 plasma raised the nitrogen to silicon ratio and/or formed the Si–H bond at the interface region as discussed previously. The number of the silicon dangling bond is decreased after plasma bombardment, which leads to the reduction of trapping electron. Therefore, during the TDDB test, the leakage current of SiN_x films with plasma bombardment increases slightly before the breakdown. The initial increase and then decrease of leakage current were not observed for SiN_x with plasma bombardment. However, the relationships of shorter TDDB lifetime and larger breakdown field (E_0) of SiN_x films with plasma bombardment are not well understood. There are many factors which degrade the TDDB lifetime. When the behavior of the current becomes more and more dominated by the conduction in band edges, and the number of defects in the band edges become too large, the breakdown occurs [13]. It is possible the plasma treated SiN_x films with less neutral states (Si_3^0) easily result in conduction in band edges, and therefore it decreases the TDDB lifetime. The plasma-treated samples have higher concentration of the weaker Si–H bonds which lead to shorter TDDB lifetime, nevertheless, the smoother surface can decrease the local shortcuts between top and bottom electrodes, resulting in higher E_0.

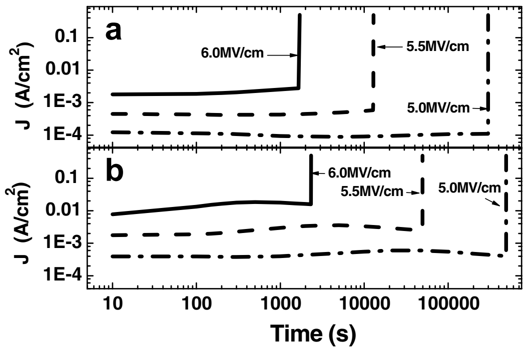

Fig. 6. Time dependence of the current density of SiN_x MIM capacitors as function of the electric field of 6.0 MV/cm, 5.5 MV/cm, and 5.0 MV/cm with (a) and without (b) plasma treatment. Failure time (T_F) versus electrical field (E) of SiN_x MIM capacitors with (circle) and without (square) plasma treatment.

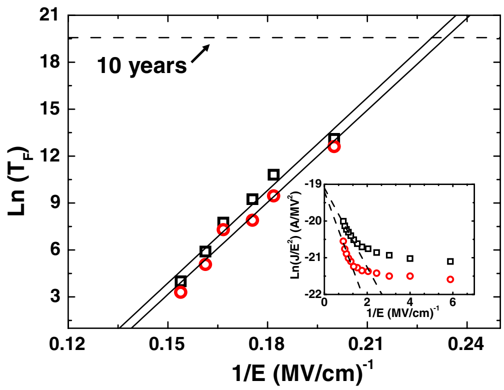

Fig. 7. Failure time (T_F) versus $1/E$ of SiN_x MIM capacitors with (circle) and without (square) plasma treatment. The inset shows the leakage current can be fitted to Fowler–Nordheim conduction at the high electric field.

The inset in Fig. 7 shows the leakage current can be fitted to Fowler–Nordheim conduction at the high electric field. Therefore, the $1/E$-model shows the $\ln(T_F)$ dependence on $1/E$ due to Fowler–Nordheim (F–N) current conduction [14]. $\ln(T_F)$ is plotted as a function of $1/E$, as shown in Fig. 7. These $\ln(T_F)$ data are fitted with $1/E$-model. These straight lines indicate possible extrapolations for the lifetime of SiN_x capacitors. The $E_{1/E\text{-model}}$ represents the extrapolated electric fields for 10 years lifetime. The $E_{1/E\text{-model}}$ is 4.26 MV/cm and 4.35 MV/cm with and without plasma treatment, respectively.

4. Conclusions

In this study, Weibull distribution function is employed to analyze the electrode area effect on the breakdown strength of the SiN_x MIM capacitors. The Weibull distribution function fits the experimental data well and this suggests that the breakdown of the dielectric can be explained with the weakest-link theory, since Weibull distribution function is based on the weakest-link theory. For SiN_x MIM capacitors, the characteristic field E_0 decreases with the increase of the electrode area (A) as predicted by the weakest-link theory. No apparent correction is observed between the Weibull slope parameter and the electrode area. Plasma treatment increases both m and E_0 of the SiN_x MIM capacitors which show smoother surface and better fitting as Eq. (7) predicated. The enhancement of SiN_x capacitors may be resulted from the decrease of trap density caused by NH_3 plasma as revealed in previous work. The plasma-treated samples have higher concentration of the weaker Si–H bonds which lead to the shorter lifetime (T_F). Both of the as-deposited SiN_x and plasma-treatment SiN_x capacitors show the longer lifetime than 10 years about 4.35 MV/cm and 4.26 MV/cm, respectively.

Acknowledgement

This work is sponsored by National Science Council, Taiwan, under the contract number NSC 93-2216-E-009-023.

References

[1] E. Wu, E. Nowak, A. Vayshenker, J. McKenna, D. Harmon, R.P. Vollertsen, IEEE Trans. Device Mater. Reliab. 1 (2001) 69.
[2] J.C. Lee, J.C. Chen, C. Hu, IEEE Trans. Electron Devices 35 (1988) 2268.
[3] D.J. DiMaria, E. Cartier, D. Arnold, J. Appl. Phys. 73 (1993) 3367.
[4] J.H. Stathis, in: Symposium on IEEE International Reliability Physics, 2001, pp. 132.
[5] J.H. Stathis, J. Appl. Phys. 86 (1999) 5757.
[6] R. Degraeve, P.H. Roussel, G. Groeseneken, H.E. Maes, Microelectron. Reliab. 36 (1999) 1639.
[7] J. Sune, IEEE Electron Device Lett. 22 (2001) 296.
[8] H.D. Su, B.S. Chiou, S.Y. Wu, M.H. Chang, K.H. Lee, Y.S. Chen, C.P. Chao, Y.C. See, Y.C. Sun, Jpn. J. Appl. Phys. 42 (2003) 5521.
[9] H.D. Su, B.S. Chiou, C.Y. Kao, S.Y. Wu, M.H. Chang, K.H. Lee, C.P. Chao, Y.C. See, Y.C. Sun, Jpn. J. Appl. Phys. 42 (2003) 7232.
[10] K.H. Allers, Microelectronics Reliab. 44 (2004) 411.
[11] C.C. Ho, B.S. Chiou, J. Mater. Sci. 42 (2007) 941.
[12] M. OhringReliability and Failure of Electronic Materials Devices, vols. 310–328, Academic Press Ltd., San Diego, CA, 1998.
[13] M.H.W.M. van Delden, P.J. van der Wel, in: Proceedings of the 41st International Reliability Physics Symp, (March). Dallas, USA, 2003, pp. 293.
[14] A.M. Yassine, H.E. Nariman, M. Mcbride, M. Uzer, K.R. Olasupo, IEEE Trans. Electron Devices 47 (2000) 1416.